IOP PUBLISHING NANOTECHNOLOGY

Nanotechnology 23 (2012) 344001 (11pp) doi:10.1088/0957-4484/23/34/344001

Multifunctional, flexible electronic systems based on engineered nanostructured materials

Hyunhyub Ko[1,2,3,4], **Rehan Kapadia**[1,2,3], **Kuniharu Takei**[1,2,3], **Toshitake Takahashi**[1,2,3], **Xiaobo Zhang**[1,2,3] and **Ali Javey**[1,2,3]

[1] Department of Electrical Engineering and Computer Sciences, University of California at Berkeley, CA 94720, USA
[2] Berkeley Sensor and Actuator Center, University of California at Berkeley, CA 94720, USA
[3] Materials Sciences Division, Lawrence Berkeley National Laboratory, Berkeley, CA 94720, USA
[4] School of Nano-Bioscience and Chemical Engineering, KIER-UNIST Advanced Center for Energy, Ulsan National Institute of Science and Technology (UNIST), Ulsan 689-798, Korea

E-mail: ajavey@eecs.berkeley.edu

Received 13 February 2012, in final form 25 April 2012
Published 10 August 2012
Online at stacks.iop.org/Nano/23/344001

Abstract

The development of flexible electronic systems has been extensively researched in recent years, with the goal of expanding the potential scope and market of modern electronic devices in the areas of computation, communications, displays, sensing and energy. Uniquely, the use of soft polymeric substrates enables the incorporation of advanced features beyond mechanical bendability and stretchability. In this paper, we describe several functionalities which can be achieved using engineered nanostructured materials. In particular, reversible binding, self-cleaning, antireflective and shape-reconfigurable properties are introduced for the realization of multifunctional, flexible electronic devices. Examples of flexible systems capable of spatial mapping and/or responding to external stimuli are also presented as a new class of user-interactive devices.

(Some figures may appear in colour only in the online journal)

1. Introduction

Over the past several decades, the continuous growth of the microelectronics industry has relied on silicon-based devices. The requirements for faster, cheaper and more energy-efficient electronics have fueled the continued progress of silicon integrated circuits [1–4]. Besides efforts to improve the performance of computer chips which are based on hard and brittle substrates, there have been tremendous efforts to develop electronic devices based on mechanically flexible substrates [5–9]. Flexible electronics, which can be bent, rolled and stretched into arbitrary shapes, would significantly expand the applications of modern electronic devices in the areas of computation, communications, displays, sensing, and energy harvesting and storage.

The progress of flexible electronics has been driven primarily by the requirement of cheaper, large-area electronic devices that can be integrated on flexible substrates through low-temperature deposition or solution-based printing methods [6, 10]. Although many promising results have been reported with organic semiconductors, the performance and lifetime of such devices suffer from low carrier mobility and poor chemical stability, which hinders their use for most electronic applications [11–13]. On the other hand, inorganic semiconductors provide superior carrier mobility and chemical stability [14]. However, the great challenge lies in integrating brittle inorganic semiconductors on flexible substrates while preserving the structural and electrical properties. Recent progress in inorganic nanomaterials process technology has largely addressed this challenge. For example, single-crystalline inorganic nanowires can be integrated

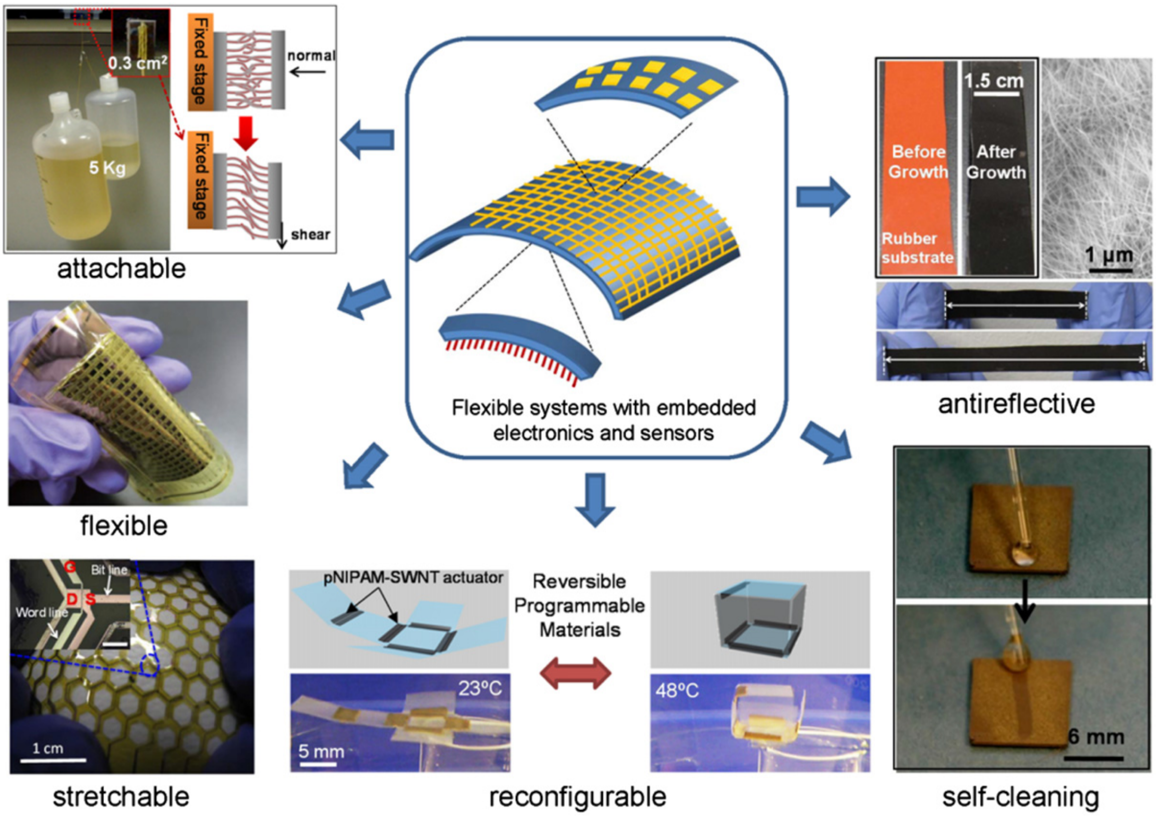

Figure 1. Multifunctional, flexible electronic systems based on engineered nanostructured materials. Reprinted with permission from [24, 42, 48, 66, 85, 97]. (Copyright 2009, 2010, 2011, American Chemical Society; Copyright 2010 Nature Publishing Group; Copyright 2009 John Wiley and Sons, Inc.)

on flexible substrates through printing or solution-based assembly methods [15]. In another example, transfer methods of micro- and nanometer thick inorganic thin films onto a wide range of substrates including silicon, glass and plastic have been demonstrated [5, 7–9]. Because the size of integrated semiconductors is on the scale of micro- to nanometers, the bending of flexible devices does not affect the mechanical stability of inorganic semiconductors.

While mechanical flexibility in electronic devices would enable new applications previously incompatible with conventionally integrated circuits, multifunctional properties are required for diverse and new applications. For example, one could imagine a mobile device which could not only bend and stretch into an arbitrary shape, but also attach to any surface, utilize an antireflective surface for efficient solar panels and displays, exhibit superhydrophobicity and self-cleaning capability, while being responsive to external stimuli. In this paper, we review the recent developments of multifunctional electronic devices. In particular, stretchable, attachable, self-cleaning, antireflective and reconfigurable functions will be introduced as potential capabilities for flexible devices (figure 1). Here, we primarily focus on the use of one-dimensional nanomaterials (e.g. nanotubes and nanowires) which offer excellent mechanical, electrical and optical properties, and can be readily grown on a wide range of substrates with tailored chemical composition.

2. Mechanically flexible devices

Flexible electronics with the capabilities of bending around curved surfaces have potential applications in rollable photovoltaics for easy installation [16–18], displays [19, 20], lighting [21], radio-frequency identification (RFID) tags [22], sensors [23] and electronic skins for robotics and prosthetics [24, 25]. The revolution of flexible electronics started with the development of organic electronic devices which possess the great advantages of low-temperature and large-area processing, and mechanical flexibility [26]. However, even with these attractive properties, the poor performance and reliability of organic electronics have shifted the research focus to inorganic semiconductors. Dramatic progress has been made in integrating inorganic nanowires (NWs) on flexible substrates through solution-flow-assisted assembly [27, 28], Langmuir–Blodgett [29, 30] and transfer printing of nanoribbons, nanowires and membranes [5, 31–33]. In particular, transfer printing methods have enabled the transfer of single-crystalline semiconductor nanostructures (X) on arbitrary substrates (Y) including rubber, plastic, metal-foil, glass and Si substrates. This X-on-Y (XoY) scheme is applicable to a wide range of material systems and device applications [34].

As an example system, figure 2(a) shows a flexible electronic skin (e-skin) device based on NW active-matrix circuitry consisting of 19 pixels × 18 pixels [24]. Figure 2(b)

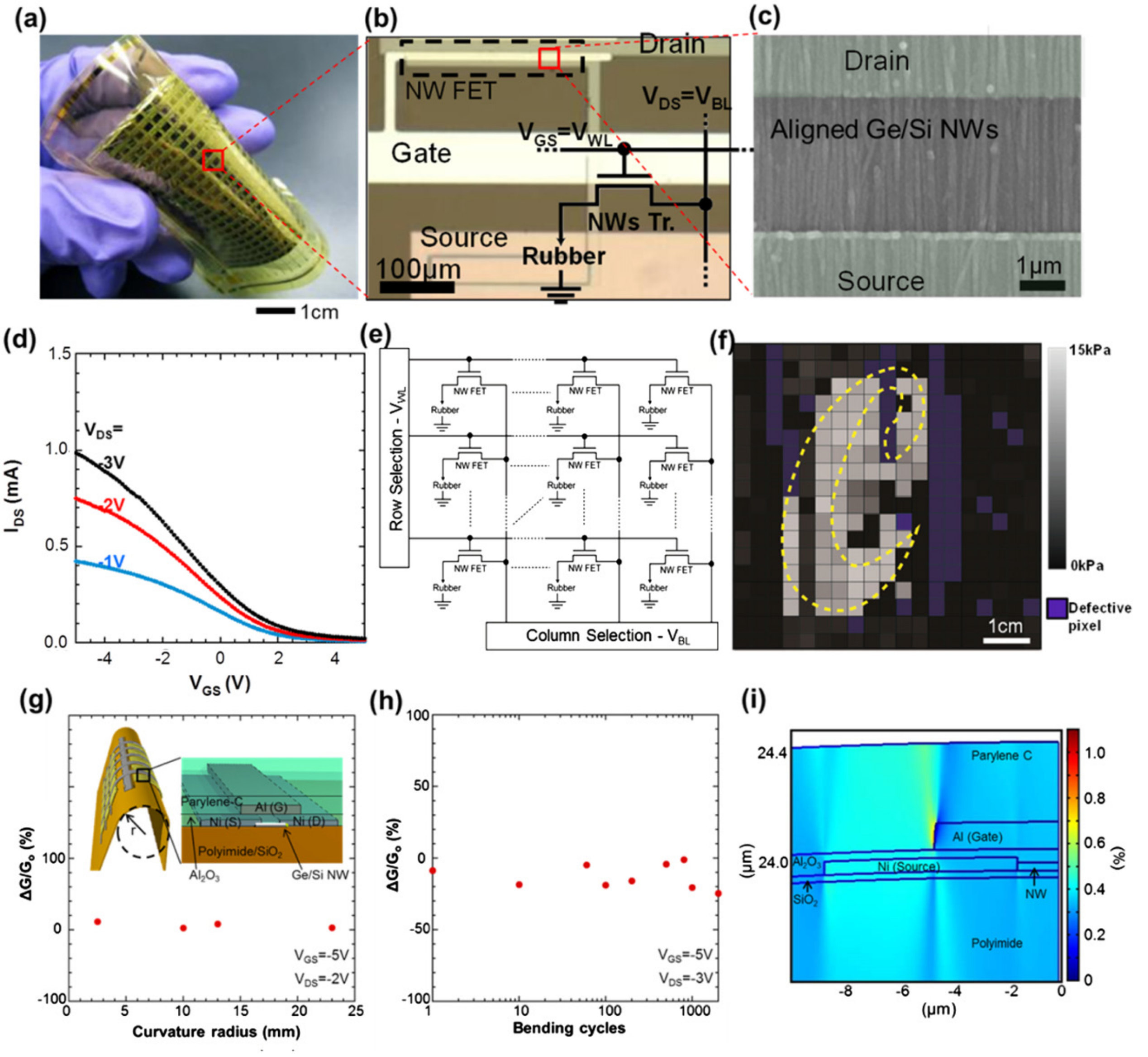

Figure 2. Flexible electronic skin (e-skin) with NW-array active-matrix circuitry. (a) A fully fabricated e-skin device (7×7 cm^2 with a 19×18 pixel array) showing high mechanical flexibility. (b) Optical microscope image of a Ge/Si NW-array FET (channel length ~ 3 μm, channel width ~ 250 μm) used in each pixel of the sensor array. The circuit structure for the pixel depicts the FET structure integrated with a PSR. (c) SEM image of a NW-array FET, showing the high degree of NW alignment and uniformity (density of ~ 5 NWs μm^{-1}). (d) The $I_{DS} - V_{GS}$ characteristics of a representative NW FET on a polyimide substrate before the lamination of the PSR. (e) Circuit schematic of the active matrix to address individual pixels by applying row (VBL) and column (VWL) signals. (f) Spatial mapping of pressure by reading the pixel outputs of the e-skin corresponding to the applied local pressure distribution of a character 'C'. The conductance change of a representative pixel (g) at different curvature radii and (h) as a function of mechanical bending cycles. (i) Theoretical simulation showing the strain distribution of a NW device when bent to a 2.5 mm curvature radius. Reprinted with permission from [24] (Copyright 2010, Nature Publishing Group).

shows an optical image of a pixel where a Ge/Si NW-array field-effect transistor (FET) integrated with a commercially available pressure-sensitive rubber (PSR) is used as a pressure sensor. Here the source electrode of the FET at each pixel is connected to ground through the PSR. Figure 2(c) shows a zoom-in scanning electron microscope (SEM) image of a FET, which illustrates a uniformly aligned Ge/Si core/shell NW array between source/drain (S/D) electrodes (density of ~ 5 NWs μm^{-1}). Here the integration of highly aligned NW arrays is achieved on a flexible polyimide (PI) substrate by contact printing of CVD-grown NWs. Figure 2(d) shows representative transfer characteristics of a NW-array FET with a peak field-effect mobility of ~ 20 cm^2 V^{-1} s^{-1} on a flexible PI substrate before the lamination of the PSR. The working principle of the pressure-sensitive e-skin is based on the modulation of ON-state conductance of NW FETs by the conductance change of PSR when external pressure is applied. Since each pixel can be addressed independently by applying word- and bit-line voltages (V_{WL}, V_{BL}) to active-matrix circuitry (figure 2(e)), spatial mapping of the local distribution

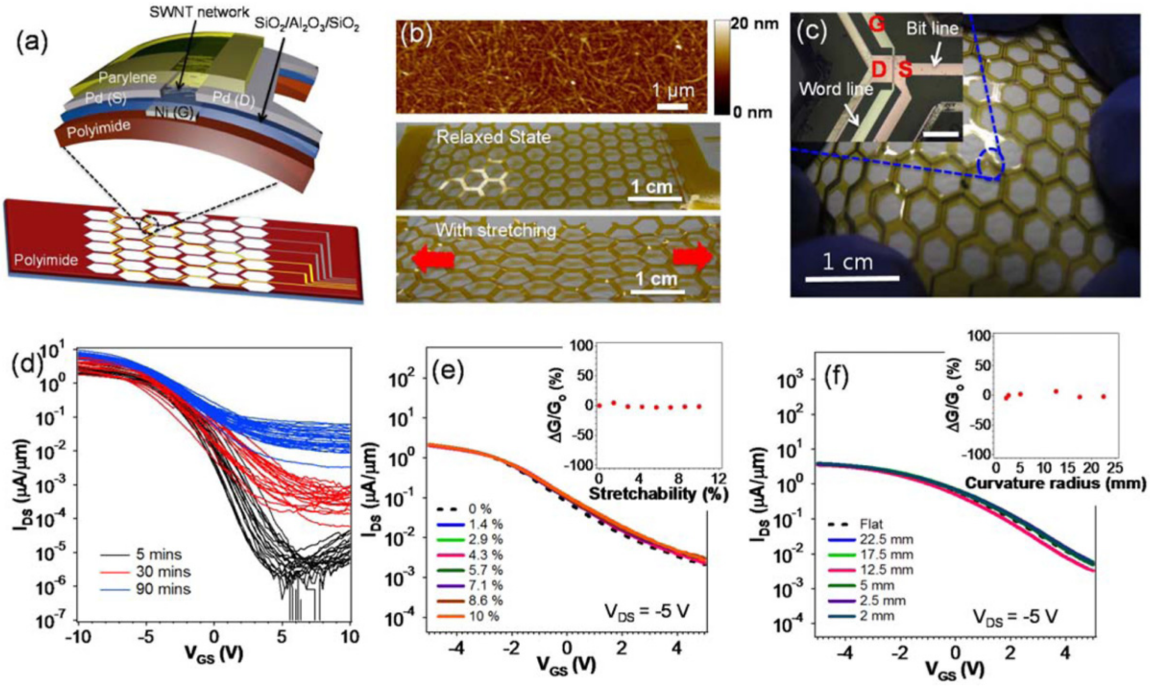

Figure 3. SWNT TFTs on mechanically stretchable substrates. (a) Schematics of mechanically flexible/stretchable SWNT TFTs used as an active-matrix backplane (6×4 cm^2 with 12×8 pixel array). (b) AFM image of SWNT networks on a PI substrate. Optical images of the honeycomb-patterned PI substrate in the relaxed and stretched states are also shown. (c) Optical images of a stretchable device array, showing conformal coverage on a baseball. Expanded image of a single pixel containing a SWNT TFT is shown in the inset (scale bar is 200 μm). (d) $I_{DS} - V_{GS}$ transfer characteristics of SWNT TFTs at $V_{DS} = -5$ V for three different SWNT deposition times of 5, 30 and 90 min, corresponding to different nanotube densities. (e) $I_{DS} - V_{GS}$ transfer characteristics at $V_{DS} = -5$ V as a function of stretchability. (f) $I_{DS} - V_{GS}$ transfer characteristics at $V_{DS} = -5$ V measured at various bending radius. Reprinted with permission from [42] (Copyright 2011, American Chemical Society.)

of pressure with a character 'C' is successfully demonstrated as shown in figure 2(f). This result demonstrates that a macroscale and low-power pressure-sensitive e-skin could be achieved by the unique NW contact printing process. Furthermore, mechanical robustness is achieved by the use of NWs which are covered by polymeric layers on both sides. As can be seen in figures 2(g) and (h), the conductance of the devices do not degrade under large bending and repeated bending cycles up to 2000 times. This mechanical robustness is due to the minimal strain encountered by the NW devices on a PI substrate with a top parylene encapsulation layer, as evident from the mechanical simulations (figure 2(i)).

3. Stretchable devices

In addition to bending or twisting, stretchability is required for certain applications where devices must conformably cover 3D objects [35, 36]. There have been several reports covering stretchable electronics based on organic or inorganic semiconductors [7–9, 37–41]. Challenges include the delamination and/or mechanical fracture of the electronic components, including the semiconductor, metal and dielectric layers. To address this issue, several designs of stretch-tolerant structures have been suggested. One approach is to utilize a 'wavy' layout, where micro/nano-inorganic semiconductors are printed on a pre-strained PDMS substrate [8, 9]. Relaxing the substrate spontaneously leads to the formation of wavy structures due to nonlinear buckling phenomena. This enables high mechanical stretchability of the substrate without fracturing the semiconductor layer. Another approach involves the use of engineered substrates with open mesh geometry [7].

An example of the stretch-tolerant structures is highlighted in figure 3(a), which utilizes single-walled carbon nanotube (SWNT) thin film transistors (TFTs) at the bridge intersects of a hexagonal mesh substrate. The resulting substrate is a mechanically stretchable active-matrix backplane [42]. Here semiconductor-enriched SWNT networks are uniformly assembled on a PI substrate and used as the active channel material as shown in an atomic force microscope (AFM) image in figure 3(b). While the original unpatterned PI film is stiff and non-stretchable, the laser cut of the PI film into a honeycomb mesh structure enables the unidirectional stretching of the substrate (figure 3(b)). The SWNT TFTs are placed at selective sites on the patterned PI substrate corresponding to the regions with minimal induced strain. The SWNT active-matrix backplane can intimately cover curved surfaces, such as a baseball shown in figure 3(c). The use of highly semiconductor-enriched SWNTs (over 99%) enables the fabrication of TFTs with superb electrical properties (mobility of $\sim$20 cm^2 V^{-1} s^{-1} and I_{ON}/I_{OFF} of $\sim 10^4$) as depicted in figure 3(d). More noteworthy is the uniformity of TFT performances across an entire 4 inch wafer. The standard deviations of transconductance (g_m), mobility (μ), $\log(I_{\mathrm{ON}}/I_{\mathrm{OFF}})$ and threshold voltage (V_{t}) are ~11%, 17%, 11% and 3%, respectively. These represent a small variation of key device parameters, especially given that the TFT arrays are fabricated in an academic research laboratory, with most processing steps performed in a non-cleanroom environment. The mechanical stability of SWNT TFT arrays on a honeycomb structured PI substrate is also studied. The device functions without noticeable electrical degradation even when stretched up to ~3 mm displacement, corresponding to ~11.5% of stretchability (figure 3(e)), or when mechanically bent to a 2 mm radius of curvature (figure 3(f)). The concept of integrated electronics on stretch-tolerant honeycomb structures, shown in the above example, can be expanded in the future to enable multifunctional artificial e-skin by adding various active electronic and sensor device components. In addition, by tuning the laser cut pattern, further optimization of the mechanical properties of the substrate can be achieved.

4. Attachable devices

The ability to reversibly attach devices to arbitrary surfaces may provide yet another important functionality for flexible electronics. Traditional connectors rely on electrostatic, magnetic or mechanical forces to bind substrates. Most techniques used at the macroscale, such as zippers, Velcro or buttons, however, are not effective when their size scales are miniaturized to the dimensions required for practical use with thin flexible substrates. On the other hand, conventional adhesives, such as glue and tape, which can be made into thin layers, are not surface-selective and/or reversible. Synthetic gecko adhesives utilize van der Waals (vdW) interactions to achieve reversible binding to most planar surfaces [43–47]. They present a platform for attachable electronics: however, they lack specificity which may be needed for certain applications where binding to only selective areas is desired. Recently, we have demonstrated a new class of chemical connectors based on inorganic/organic core/shell NW arrays that utilize vdW interactions to enable self-selective and reversible binding [48]. As compared to synthetic gecko adhesives, NW connectors are designed to be mechanically stiff, therefore providing weak adhesion forces to planar surfaces. A strong shear adhesion is obtained only when they are engaged with self-similar, nanofibrillar surfaces [48]. In addition, the connectors can be made electrically active by coating a conducting metal layer on the outer surface of NWs to enable both physical and electrical connections simultaneously [49].

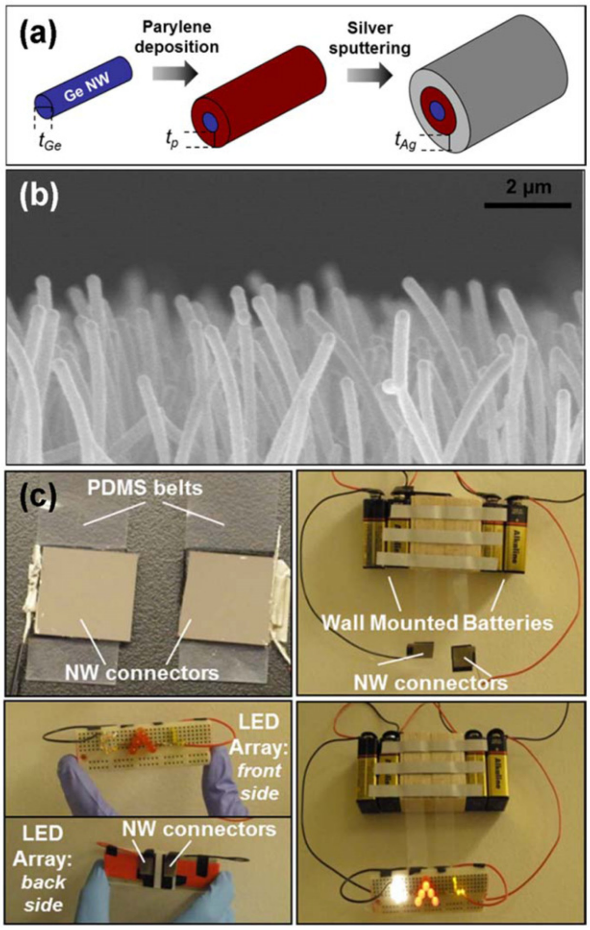

Figure 4. Electrical connectors based on Ge/parylene/Ag core–multishell hybrid NW forests. (a) Schematic illustration of the fabrication process of the core–multishell NW forests. (b) SEM image of a representative core–multishell NW forest. (c) An LED array is physically and electrically connected to a wall-mounted battery pack via NW electrical connectors. Reprinted with permission from [49]. (Copyright 2009, American Institute of Physics.)

Figures 4(a) and (b) demonstrate the structural schematic and a representative SEM image of an electrical connector based on Ge/parylene/Ag core–multishell NW arrays [49]. In this hybrid NW system, Ge NWs are used as templates for the subsequent deposition of multiple shells and provide the needed mechanical stiffness for selective binding; a parylene shell is used to enhance the surface compliance and therefore the adhesion force; and an Ag outer shell is used for enabling electrical conductivity. An example application is shown in figure 4(c), where a light-emitting diode (LED) array is electrically and physically connected to a wall-mounted battery pack by using a pair of NW connectors. The two key advantages of utilizing connectors and adhesives based on van der Waals interactions are (i) the ability to arbitrarily shrink down the size of the binding sites and (ii) the ability to maintain adhesion strength after multiple attachment and detachment cycles.

5. Self-cleaning devices

The introduction of self-cleaning surfaces on electronic devices paves the way for waterproof and dust-free electronics. For example, self-cleaning surfaces in solar panels can increase light conversion efficiency via reducing dust build-up which blocks sunlight [50]. Self-cleaning surfaces with minimal fingerprint residue are highly desirable for flexible touch pads. The inspiration for synthetic self-cleaning surfaces is found in biological systems. For example, the hierarchical micro- and nanostructured bumps on a lotus

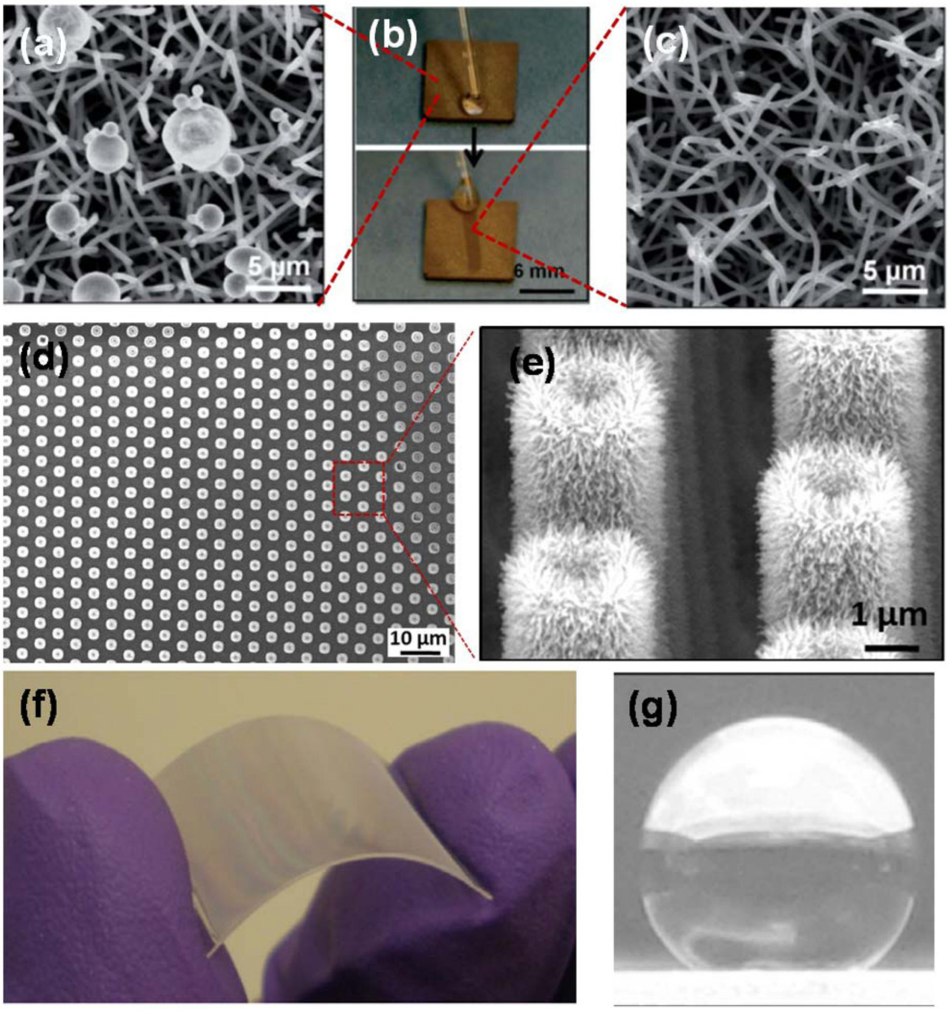

Figure 5. Self-cleaning surfaces based on superhydrophobic nanofibrillar structures. (a) Particulate contaminants on nanoscale fibrillar structures. (b) Self-cleaning of particulate contaminants by rolling a water droplet on a superhydrophobic surface. (c) A nanofibrillar surface after cleaning of particulate contaminants. (d), (e) Hierarchical μPLR/NW structures achieved by ZnO NW decoration of the PC μPLR backbones. (f) A hierarchical μPLR/NW structure with a PC supporting substrate showing mechanical flexibility. (g) A hierarchical μPLR/NW structure showing superhydrophobic properties. Reprinted with permission from [66]. (Copyright 2009, John Wiley and Sons, Inc.)

leaf provide both high water contact angle and low contact angle hysteresis, resulting in extremely water-repellent or superhydrophobic surfaces, where any dust on the surface can be easily cleaned off by the rolling raindrops [51, 52]. There have been numerous reports [53–65] covering the fundamental principles and fabrication technologies of artificial superhydrophobic surfaces. Most approaches rely on the micro- and nanoscale texturing of the surface, followed by the surface modification with low surface energy, hydrophobic chemical species such as poly(tetrafluoroethylene) (PTFE), octadecyltrichlorosilane (OTS), polystyrene and polycarbonate. Several challenges, including low cost fabrication processing techniques for large-area coverage, need to be addressed. In this regard, quasi-vertical NWs grown by CVD and/or solution-based process techniques provide a promising platform for scalable, self-cleaning surfaces [66].

As an example, self-cleaning surface characteristics of parylene/Ge NW arrays, similar to those used for the connectors, are depicted in figures 5(a)–(c). This behavior arises from the hydrophobic parylene shell combined with the nanoscale fibrillar structure of NWs. The superhydrophobic behavior can be further enhanced by using hierarchical micro/nanostructures [67, 68]. For instance, figures 5(d) and (e) show the hierarchical fibrillar arrays based on polycarbonate (PC) microscale pillars (μPLs; diameter 1.5 μm, length 10 μm, pitch 6 μm) decorated on the surface with ZnO NWs (diameter 20–30 nm, length 1.5 μm). To increase the hydrophobicity, 10 nm thick parylene-N was covered over the ZnO/PC surface. Here, the structures are fabricated by thermal micromolding of a PC polymer film on a silicon mold followed by solution-based synthesis of ZnO NWs. Since the process steps are performed at relatively low temperatures, the process scheme is compatible with most plastic substrates. As a result, mechanically flexible, superhydrophobic hierarchical surfaces can be readily obtained over large areas (figures 5(f) and (g)) for applications in flexible electronic systems with self-cleaning surfaces.

6. Antireflective devices

Antireflective surfaces have attracted much attention in modern optoelectronics for applications in displays, photovoltaics and photodetectors. For example, antireflective displays offer low reflection without affecting the screen contrast [69–71]. Antireflective surfaces in solar panels minimize light reflection and thus maximize the harvesting of solar energy [50, 72–74]. Photodetectors with antireflective layers enhance the photon sensitivity [75, 76]. Antireflective surfaces are fabricated by the deposition of multilayered thin films or the formation of tapered three-dimensional (3D) nanostructures on the target substrates [77]. Multilayer thin film approaches have limitations in broadband and wide-angle omnidirectional antireflection applications [74, 78]. In addition, the deposition of multilayer thin films with finely tuned refractive index, and the thermal stability of heterogeneous multilayer films on target substrates with different thermal expansion coefficients, present challenges for a wide range of optical wavelengths [79, 80].

The tapered three-dimensional (3D) nanostructures inspired by biological antireflective systems such as the moth's eye provide true broadband and omnidirectional antireflective surfaces [81–83]. This property arises from the gradual reduction of the effective refractive index of the tapered nanostructures from the bottom to the top surface. This property decreases the Fresnel reflection observed on planar surfaces where the large mismatch of refractive index between air and the planar material is ascribed to the large light reflection [84].

Figure 6(a) shows an SEM image of quasi-vertical Ge nanoneedles synthesized by Ni-catalyzed chemical vapor deposition [85]. The transmission electron microscope (TEM) image of a Ge nanoneedle depicts the sharp tip (~4 nm in diameter) with gradual increase of diameter towards the base. Importantly, Ge nanoneedle arrays can be directly grown on flexible substrates (e.g. polyimide and high-temperature rubber) because of the low growth temperatures (~270 °C) required for nanoneedles as shown in figure 6(b). The optical reflectance spectra of Ge materials with different morphologies including thin film (TFs), NW and nanoneedle arrays are shown in figure 6(c). The reflectance decreases from 80–90% for TFs, to 2–10% for NWs and to <1% for nanoneedle arrays. Notably, the Ge nanoneedle samples exhibit a visually black appearance due to the low reflectance. The same concept can be applied to optically transparent NWs and nanoneedles for optically transparent and antireflective surfaces.

7. Stimuli-responsive devices

Structures that reversibly change their shape, color and/or other physical and chemical properties in response to external stimuli represent an interesting class of programmable materials [86, 87]. Here, the stimuli could range from mechanical stress, light, heat, electric and magnetic fields, moisture or pH. Stimuli-responsive materials are receiving increased attention for applications in microrobotics, artificial muscles, smart actuator systems and chromic windows with tunable transparency [88–90]. Incorporating stimuli-responsive properties in flexible electronic systems could further enhance the enabled applications and functionalities. For example, chromic materials with the ability to change color or optical transparency in response to electric fields, heat or light may enable advanced flexible displays [91, 92]. In another example, recent reports have demonstrated that responsive composite layers with different mechanical moduli can be self-configured into 3D structures [93]. Such results pave the way for the development of shape-reconfigurable devices in response to external stimuli.

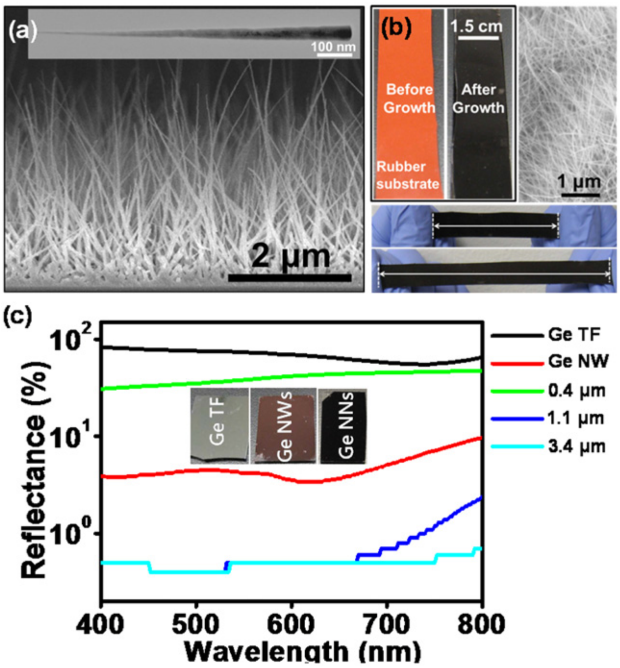

Figure 6. Black germanium with antireflective surface properties. (a) An SEM image of a representative Ge nanoneedle array with quasi-vertical geometry. The inset shows a TEM image of a nanoneedle with a tip diameter of ~4 nm. (b) Optical and SEM images of Ge nanoneedles grown on high-temperature rubber substrates. Notably, the substrate with nanoneedles exhibits a visually black appearance showing the antireflective property. The optical images at the bottom show the stretchability of the grown Ge nanoneedle arrays on a rubber substrate. (c) The reflectance spectra of Ge TF, Ge NWs ($d \sim 30$ nm, $L \sim 20$ μm) and Ge nanoneedles with different lengths. The inset shows the optical images of three representative substrates. Reprinted with permission from [85]. (Copyright 2010, American Chemical Society.)

In order to reversibly shape a substrate into a user-defined structure, stimuli-responsive actuators and adhesive systems are required to fold hinges and connect surfaces. Figure 7 shows an example of a thermo-responsive connector [94]. The connectors are based on the use of thermo-responsive poly(N-isopropylacrylamine) (pNIPAM) coatings on quasi-vertical NW arrays. pNIPAM is a hydrogel polymer which

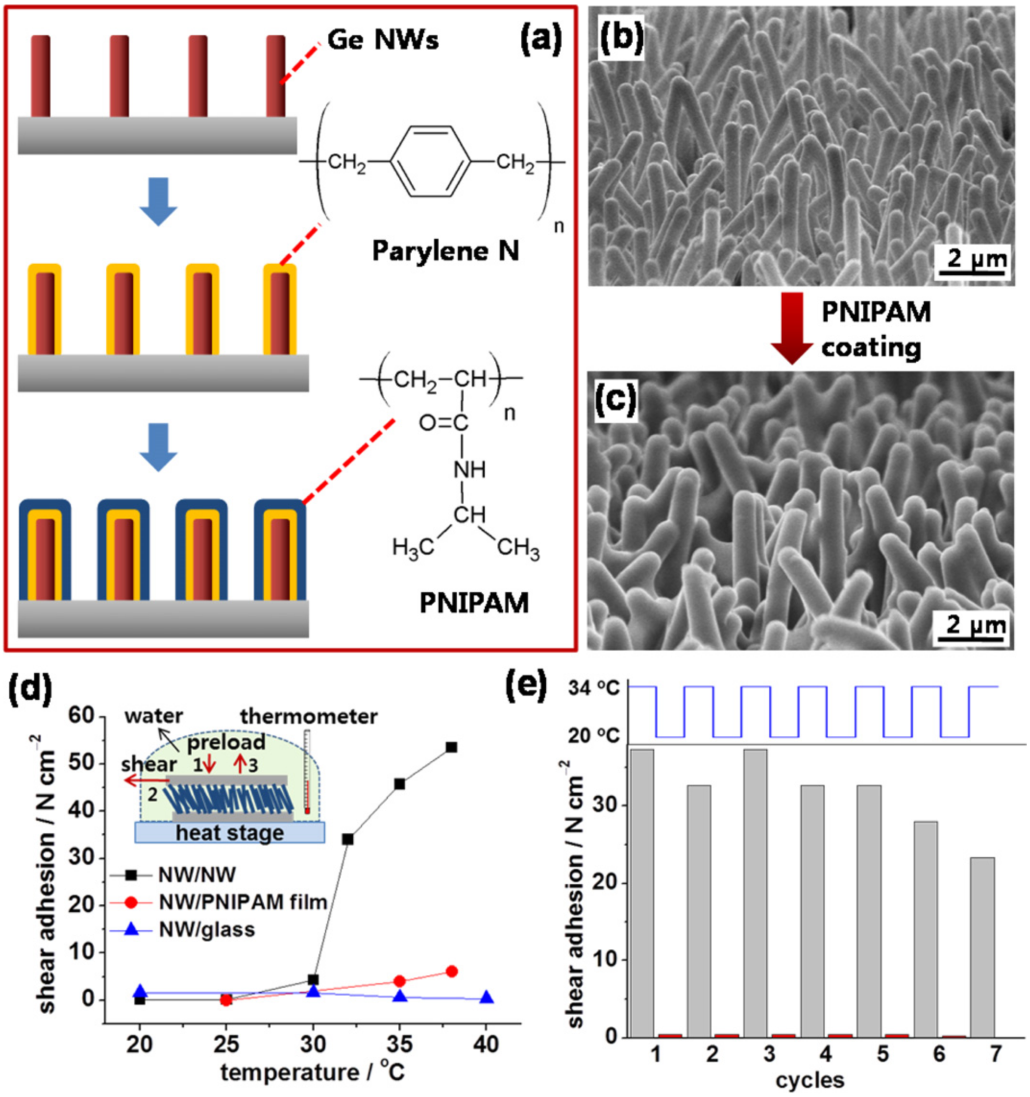

Figure 7. Thermo-responsive NW connectors. (a) Fabrication procedure for a thermo-responsive NW forest with a Ge/parylene/pNIPAM core/multishell structure. (b), (c) SEM images of Ge/parylene NW forests before and after the deposition of the pNIPAM outer shell. (d) Shear wet adhesion strengths of the thermo-responsive NW fasteners as a function of temperature. (e) Reversible modulation of shear adhesion strength is observed as the temperature is fluctuated between 20 and 34 °C. Reprinted with permission from [94]. (Copyright 2010, John Wiley and Sons, Inc.)

swells or shrinks in response to changes in temperature at the lower critical solution temperature (LCST, ∼32 °C in water) [95, 96]. Below the LCST, pNIPAM swells by absorbing water, and above the LCST, pNIPAM shrinks by expelling water. The thermo-responsive NW connectors with Ge/parylene/pNIPAM core/multishell structures are fabricated by photopolymerization of the pNIPAM shell on the NW arrays (figures 7(a)–(c)). Figure 7(d) shows the change in the shear adhesion strengths of a NW connector in water as a function of temperature. When the temperature is below the LCST, the NW connector shows minimal shear adhesion strength. However, the shear adhesion strength is significantly enhanced when the water temperature is above the LCST. More importantly, these thermo-responsive adhesion properties are fully reversible. Figure 7(e) shows the reversible switching of adhesion strength of NW connectors by alternately immersing NW connectors between high- and low-temperature water baths. The reversible change of adhesion strength is about 170× in response to a 5 °C change of water temperature. Although this work is based on the responsive surfaces on silicon substrates, this concept provides the opportunity for further explorations on flexible substrates with a wide range of stimuli-responsive materials that respond to light, electric field or environmental changes.

pNIPAM hydrogels can also be engineered for use as thermo-responsive actuators, thereby enabling the fabrication of shape-reconfigurable structures which can change shape in response to thermal stimuli. Figure 8 shows an example of shape-reconfigurable structures which mimic the closing or blossoming of a box as controlled by changes in water temperature [97]. Here, composite patches of pNIPAM hydrogels and carbon nanotubes (CNTs) are used as actuator hinges for the mechanical motion of low-density

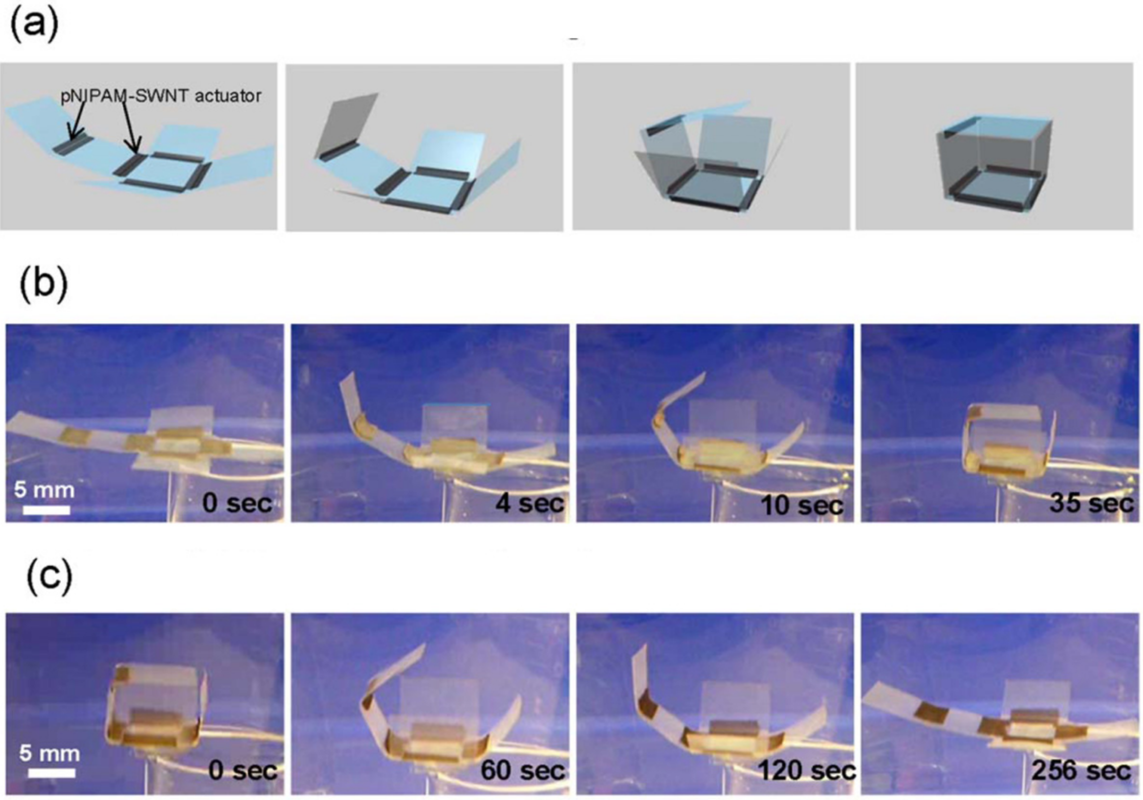

Figure 8. A shape-reconfigurable cube based on thermal-responsive actuators. (a) Schematics of folding procedures for a cube based on SWNT-loaded pNIPAM/LDPE bilayer actuators. (b) Stimuli-responsive cube folding as the water temperature is increased to 48 °C. (c) Reversible unfolding of the cube by cooling down the water bath in which the cube is immersed. Reprinted with permission from [97]. (Copyright 2011, American Chemical Society.)

polyethylene (LDPE) films. The addition of CNTs to the pNIPAM hydrogels provides a more rapid response of the actuators by ∼5× as compared to samples without CNTs. The reversible stimuli-responsive actuators present a framework for further investigation of self-reconfigurable and user-interactive systems that can respond to a wide range of external stimuli.

8. Conclusion and outlook

In this paper, we described the use of nanostructured materials to introduce multiple novel functionalities in flexible electronic systems. Besides the use as the active channel material for electronics and sensors, CNT and NW arrays can be configured to enable reversible connectivity, self-cleaning and antireflective surface properties. The work discussed in this paper sets the stage for the development of user-interactive flexible systems with advanced functionalities that detect and respond to stimuli, for instance through shape reconfiguration. There are tremendous research opportunities in the area of flexible electronics, ranging from large-scale materials development and synthesis, device processing and system integration, all of which are necessary to enable the example systems described in this paper.

Acknowledgments

This work was supported by NSF, DARPA, COINS and BSAC. AJ acknowledges a Sloan Research Fellowship, NSF CAREER Award, and support from the World Class University program at Sunchon National University. RK acknowledges an NSF Graduate Fellowship. HK acknowledges support from the National Research Foundation of Korea (no. 2011-0014965), KIST (no. 2E22112-11-249) and 2010 research fund of UNIST.

References

[1] Ferain I, Colinge C A and Colinge J-P 2011 *Nature* **479** 310
[2] Lundstrom M 2003 *Science* **299** 210
[3] Theis T N and Solomon P M 2010 *Science* **327** 1600
[4] Chau R, Doyle B, Datta S, Kavalieros J and Zhang K 2007 *Nature Mater.* **6** 810
[5] Sun Y and Rogers J A 2008 *Adv. Mater.* **19** 1897
[6] Forrest S R 2004 *Nature* **428** 911
[7] Sekitani T and Someya T 2010 *Adv. Mater.* **22** 2228
[8] Kim D-H, Xiao J, Song J, Huang Y and Rogers J A 2010 *Adv. Mater.* **22** 2108
[9] Rogers J A, Someya T and Huang Y 2010 *Science* **327** 1603
[10] Roncali J, Leriche P and Cravino A 2007 *Adv. Mater.* **19** 2045
[11] Ma H, Yip H-L, Huang F and Jen A K-Y 2010 *Adv. Funct. Mater.* **20** 1371
[12] Service R F 2000 *Science* **287** 415

[13] Abbel R, Woffs M, Bovee R A A, van Dongen J L J, Lou X, Henze O, Feast W J, Meijer E W and Schenning A P H J 2009 *Adv. Mater.* **21** 597
[14] Heyns M and Tsai W 2009 *MRS Bull.* **34** 485
[15] Fan Z, Ho J C, Takahashi T, Yerushalmi R, Takei K, Ford A C, Chueh Y-L and Javey A 2009 *Adv. Mater.* **21** 3730
[16] Krebs F C, Gevorgyan S A and Alstrup J 2009 *J. Mater. Chem.* **19** 5442
[17] Krebs F C, Jørgensen M, Norrman K, Hagemann O, Alstrup J, Nielsen T D, Fyenbo J, Larsen K and Kristensen J 2009 *Sol. Energy Mater. Sol. Cells* **93** 422
[18] Fan Z *et al* 2009 *Nature Mater.* **8** 648
[19] Gelinck G H *et al* 2004 *Nature Mater.* **3** 106
[20] Mach P, Rodriguez S J, Nortrup R, Wiltzius P and Rogers J A 2001 *Appl. Phys. Lett.* **78** 3592
[21] Gustafsson G, Cao Y, Treacy G M, Klavetter F, Colaneri N and Heeger A J 1992 *Nature* **357** 477
[22] Cantatore E, Geuns T C T, Gelinck G H, van Veenendaal E, Gruijthuijsen A F A, Schrijnemakers L, Drews S and de Leeuw D M 2007 *IEEE J. Solid-State Circuits* **42** 84
[23] Lumelsky V J, Shur M S and Wagner S 2001 *IEEE Sensors J.* **1** 41
[24] Takei K, Takahashi T, Ho J C, Ko H, Gillies A G, Leu P W, Fearing R S and Javey A 2010 *Nature Mater.* **9** 821
[25] Someya T, Sekitani T, Iba S, Kato Y, Kawaguchi H and Sakurai T 2004 *Proc. Natl Acad. Sci.* **101** 9966
[26] Garnier F, Hajlaoui R, Yassar A and Srivastava P 1994 *Science* **265** 1684
[27] Duan X, Niu C, Sahi V, Chen J, Parce J W, Empedocles S and Goldman J L 2003 *Nature* **425** 274
[28] McAlpine M C, Friedman R S, Jin S, Lin K-H, Wang W U and Lieber C M 2003 *Nano Lett.* **3** 1531
[29] Jin S, Whang D M, McAlpine M C, Friedman R S, Wu Y and Lieber C M 2004 *Nano Lett.* **4** 915
[30] Tao A, Kim F, Hess C, Goldberger J, He R R, Sun Y G, Xia Y N and Yang P D 2003 *Nano Lett.* **3** 1229
[31] Menard E, Lee K J, Khang D-Y, Nuzzo R G and Rogers J A 2004 *Appl. Phys. Lett.* **84** 5398
[32] Ahn J-H, Kim H-S, Lee K J, Jeon S, Kang S J, Sun Y, Nuzzo R G and Rogers J A 2006 *Science* **314** 1754
[33] Fan Z, Ho J C, Jacobson Z A, Yerushalmi R, Alley R L, Razavi H and Javey A 2008 *Nano Lett.* **8** 20
[34] Madsen M, Takei K, Kapadia R, Fang H, Ko H, Takahashi T, Ford A C, Lee M H and Javey A 2011 *Adv. Mater.* **23** 3115
[35] Viventi J *et al* 2011 *Nature Neurol.* **14** 1599
[36] Kim D-H *et al* 2011 *Science* **333** 838
[37] Lacour S P, Jones J, Wagner S, Li T and Suo Z 2005 *Proc. IEEE* **93** 1459
[38] Khang D-Y, Jiang H, Huang Y and Rogers J A 2006 *Science* **311** 208
[39] Kim D-H, Ahn J-H, Won M C, Kim H-S, Kim T-H, Song J, Huang Y Y, Liu Z, Lu C and Rogers J A 2008 *Science* **320** 507
[40] Sekitani T, Noguchi Y, Hata K, Fukushima T, Aida T and Someya T 2008 *Science* **321** 1468
[41] Sekitani T, Nakajima H, Maeda H, Fukushima T, Aida T, Hata K and Someya T 2009 *Nature Mater.* **8** 494
[42] Takahashi T, Takei K, Gillies A G, Fearing R S and Javey A 2011 *Nano Lett.* **11** 5408
[43] Arzt E, Gorb S and Spolenak R 2003 *Proc. Natl Acad. Sci. USA* **100** 10603
[44] Murphy M, Aksak B and Sitti M 2007 *J. Adhes. Sci. Technol.* **21** 1281
[45] Zhao Y, Tong T, Delzeit L, Kashani A, Meyyappan M and Majumdar A 2006 *J. Vac. Sci. Technol.* B **24** 331
[46] Qu L and Dai L 2007 *Adv. Mater.* **19** 3844
[47] Lee J, Fearing R S and Komvopolous K 2008 *Appl. Phys. Lett.* **93** 191910
[48] Ko H, Lee J, Schubert B E, Chueh Y L, Leu P W, Fearing R S and Javey A 2009 *Nano Lett.* **9** 2054
[49] Kapadia R, Ko H, Chueh Y-L, Ho J C, Takahashi T, Zhang Z and Javey A 2009 *Appl. Phys. Lett.* **94** 263110
[50] Zhu J, Hsu C-M, Yu Z, Fan S and Cui Y 2010 *Nano Lett.* **10** 1979
[51] Barthlott W and Neinhuis C 1997 *Planta* **202** 1
[52] Blossey R 2003 *Nature Mater.* **2** 301
[53] Lafuma A and Quere D 2003 *Nature Mater.* **2** 457
[54] Sun T L, Feng L, Gao X F and Jiang L 2005 *Acc. Chem. Res.* **38** 644
[55] Li X M, Reinhoudt D and Crego-Calama M 2007 *Chem. Soc. Rev.* **36** 8
[56] Ma M L and Hill R M 2006 *Curr. Opin. Colloid Interface Sci.* **11** 193
[57] Bharat B 2009 *Phil. Trans. R. Soc.* A **367** 1445
[58] Lau K K S, Bico J, Teo K B K, Chhowalla M, Amaratunga G A J, Milne W I, McKinley G H and Gleason K K 2003 *Nano Lett.* **3** 1701
[59] Erbil H Y, Demirel A L, Avci Y and Mert O 2003 *Science* **299** 1377
[60] Bravo J, Zhai L, Wu Z Z, Cohen R E and Rubner M F 2007 *Langmuir* **23** 7293
[61] Furstner R, Barthlott W, Neinhuis C and Walzel P 2005 *Langmuir* **21** 956
[62] Chiou N R, Lui C M, Guan J J, Lee L J and Epstein A J 2007 *Nature Nanotechnol.* **2** 354
[63] Koch K, Bhushan B, Jung Y C and Barthlott W 2009 *Soft Matter* **5** 1386
[64] Shieh J, Hou F J, Chen Y C, Chen H M, Yang S P, Cheng C C and Chen H L 2010 *Adv. Mater.* **22** 597
[65] Verho T, Bower C, Andrew P, Franssila S, Ikkala O and Ras R H A 2011 *Adv. Mater.* **23** 673
[66] Ko H, Zhang Z, Chueh Y-L, Ho J C, Lee J, Fearing R S and Javey A 2009 *Adv. Funct. Mater.* **19** 3098
[67] Nosonovsky M and Bhushan B 2008 *Adv. Funct. Mater.* **18** 843
[68] Zhu L, Xiu Y, Xu J, Tamirisa P A, Hess D W and Wong C-P 2005 *Langmuir* **21** 11208
[69] Liu X, Cai X, Mao J and Jin C 2001 *Appl. Surf. Sci.* **183** 103
[70] Ho J-J, Chen C-Y, Huang C-M, Lee W J, Liou W-R and Chang C-C 2005 *Appl. Opt.* **44** 6176
[71] Hoshino T, Itoh M and Yatagai T 2007 *Appl. Opt.* **46** 648
[72] Prevo B G, Hon E W and Velev O D 2007 *J. Mater. Chem.* **17** 791
[73] Koynov S, Brandt M S and Stutzmann M 2006 *Appl. Phys. Lett.* **88** 203107
[74] Lee Y J, Ruby D S, Peters D W, McKenzie B B and Hsu J W P 2008 *Nano Lett.* **8** 1501
[75] Lien W-C, Tsai D-S, Chiu S-H, Senesky D G, Maboudian R, Pisano A P and He J-H 2011 *IEEE Electron Device Lett.* **32** 1564
[76] Zhou Q, McIntosh D C, Chen Y, Sun W, Li Z and Campbell J C 2011 *Opt. Exp.* **19** 23664
[77] Li Y, Zhang J and Yang B 2010 *Nano Today* **5** 117
[78] Kuo M-L, Poxson D J, Kim Y S, Mont F W, Kim J K, Schubert E F and Lin S-Y 2008 *Opt. Lett.* **33** 2527
[79] KiKuta H, Toyota H and Yu W 2003 *Opt. Rev.* **10** 63
[80] Min W-L, Betancourt A P, Jiang P and Jiang B 2008 *Appl. Phys. Lett.* **92** 141109
[81] Huang Y-F *et al* 2007 *Nature Nanotechnol.* **2** 770
[82] Clapham P B and Hutley M C 1973 *Nature* **244** 281
[83] Chen Q, Hubbard G, Shields P A, Liu C, Allsopp D W E, Wang W N and Abbott S 2009 *Appl. Phys. Lett.* **94** 263118
[84] Wilson S J and Hutley M C 1982 *Opt. Acta* **29** 993
[85] Chueh Y-L *et al* 2010 *Nano Lett.* **10** 520
[86] Stuart M A C *et al* 2010 *Nature Mater.* **9** 101

[87] Roy D, Cambre J N and Sumerlin B S 2010 *Prog. Polym. Sci.* **35** 278
[88] Shankar R, Ghosh T K and Spontak R J 2007 *Soft Matter* **3** 1116
[89] Ratna D and Karger-Kocsis J 2008 *J. Mater. Sci.* **43** 254
[90] Willner I, Basnar B and Willner B 2007 *Adv. Funct. Mater.* **17** 702
[91] Rosseinsky D R and Mortimer R J 2001 *Adv. Mater.* **13** 783
[92] Argun A A, Aubert P-H, Thompson B C, Schwendeman I, Gaupp C L, Hwang J, Pinto N J, Tanner D B, MacDiarmid A G and Reynolds J R 2004 *Chem. Mater.* **16** 4401
[93] Bassik N, Stern G M, Jamal M and Gracias D H 2008 *Adv. Mater.* **20** 4760
[94] Ko H, Zhang Z, Chueh Y-L, Saiz E and Javey A 2010 *Angew. Chem. Int. Edn* **49** 616
[95] Schild H G 1992 *Prog. Polym. Sci.* **17** 163
[96] Liang L, Feng X, Liu J, Rieke P C and Fryxell G E 1998 *Macromolecules* **31** 7845
[97] Zhang X *et al* 2011 *Nano Lett.* **11** 3239